Astron. Astrophys. 188, 183–197 (1987)

ASTRONOMY
AND
ASTROPHYSICS

Properties of solar magnetic fluxtubes from only two spectral lines

S.K. Solanki, C. Keller, and J.O. Stenflo

Institute of Astronomy, ETH-Zentrum, CH-8092 Zürich, Switzerland

Received May 11, accepted May 19, 1987

Summary. A procedure requiring only the Stokes V and Q profiles of two spectral lines (Fe I 5250.2 Å and Fe I 5247.1 Å) to determine magnetic field strength, velocity and temperature inside solar magnetic fluxtubes, as well as their inclinations and filling factors with a minimum of a priori assumptions is presented. The individual diagnostic steps of the procedure are analytically and numerically investigated. Thus the dependence of the Stokes Q σ-π asymmetry, Stokes V and Q 5250/5247 line ratio, and V/Q ratio on the angle of the field to the line of sight, temperature, limb distance, magnetic field strength, microturbulence and macroturbulence velocity are examined. It is also demonstrated that whereas the integrated V profile is a good approximation for Stokes I in magnetic regions for all lines with small Zeeman splitting, this is the case for the (doubly integrated) Q and U profiles only for very weak lines.

The procedure is then applied to spectra of the two lines obtained at various distances from the solar limb. Some results: A considerable velocity broadening is required at all positions on the disk to reproduce the polarimeter data (Stokes V line width). The centre to limb variation (CLV) of the 5250/5247 Stokes V and Q line ratios is shown to contain little information on the height variation of the magnetic field in the context of one dimensional models. The plage model of Solanki (1986) reproduces the CLV of the very temperature sensitive Stokes Q asymmetry reasonably well. The fluxtubes in half of the observed regions are inclined by at least 10° to the vertical (from the Q/V ratio). Finally, the filling factors are determined, taking into account the line weakening, inclination of the field, and an estimate of the CLV of the fluxtube continuum contrast.

Key words: solar magnetic fields – active regions – fluxtubes – Stokes parameters – diagnostics

1. Introduction

Most of our present knowledge on the internal structure of the spatially unresolved fluxtubes has been derived from spectroscopic observations in polarized light. Although the process of extracting the information from the data is quite involved and often relies heavily on model calculations, it has been possible to find lines or groups of lines with parameters which depend only on one fluxtube property or are otherwise easily interpretable. Diagnostic techniques based on such parameters include both "few-lines methods" involving one or at the most a few spectral lines (line ratio for temperature, Harvey and Livingston, 1969; line ratio for magnetic field, Stenflo, 1973; single line Fourier technique for magnetic field, Title and Tarbell, 1975; etc.) and 'many-lines methods' involving the statistical analysis of a large number of lines (e.g. Solanki and Stenflo, 1984, 1985; Solanki, 1986). The respective advantages and disadvantages of the two approaches to the data analysis have been reviewed by Solanki (1987a), who came to the conclusion that many- and few-lines analyses complement each other rather well. The advantages of few-lines techniques include that they can be applied to a larger variety of data and they are considerably less intensive in computing time.

In the present paper we concentrate on few-lines methods. In the first half of the paper we develop and investigate diagnostic techniques requiring only one or two lines, both analytically and with the help of model calculations. In the second half we apply them to solar data in an illustrative example. Our aim is to find a way of consistently determining the magnetic field strength, velocity, temperature, inclination, and filling factor of the fluxtubes in the resolution element using the V and Q profiles of only two (carefully selected) spectral lines under a minimum of a priori assumptions.

The basic idea of tackling this problem is the following: We choose the well known pair of lines. Fe I 5250.2 Å ($g = 3$, $\chi_e = 0.12$ eV, $\log gf = -4.938$) and Fe I 5247.1 Å ($g_{\rm eff} = 2$, $\chi_e = 0.09$ eV, $\log gf = -4.946$), which allow the magnetic field to be determined in a rather model independent manner through their line ratio (Stenflo, 1973). The $\log gf$ values have been taken from Blackwell et al. (1979). We follow an iterative procedure, with each iteration being composed of a number of steps. In a first step we determine the velocity inside the fluxtubes by fitting the width of the less Zeeman broadened 5247.1 Å line via comparison with a synthetic V profile calculated assuming a vertical fluxtube with temperature and magnetic field structure derived from the literature. For the velocity broadening we use the simple macro- and microturbulence approach, although a more sophisticated mechanism may also be applied if so desired. Then we determine the magnetic field strength from the line ratio. Since, besides B, the line ratio depends most strongly on velocity broadening, we can iterate these two steps until the widths of both Stokes V profiles and their amplitude ratio are simultaneously reproduced. In the next step we determine the temperature from the asymmetry between the areas of the σ- and π-components of Stokes Q. Although, as we shall see in Sect. 2, the Stokes Q

Send offprint requests to: S.K. Solanki

σ-π-asymmetry depends not only on the temperature, but also on the magnetic field strength and the velocity broadening, this is not a major drawback, since both B and the velocity have been determined in the first two steps. Next, the angle of the magnetic field to the line of sight, γ, is derived (under the assumption of azimuthal angle $\chi = 0°$) from the Q/V ratio. If observations of U were also available, then this technique could easily be extended to determine the true inclination angle from Q/U and Q/V, which together give χ and γ. Once χ and γ, and the angle between the line of sight and the vertical, θ, are known we can determine the angle of inclination of the fluxtubes with respect to the solar surface. Then, using the new angle of inclination of the field we start once more at step 1 and repeat the procedure until we reach convergence. Our experience has shown that this is quite rapid. Finally, the filling factor can be determined using the other quantities calculated so far and the observed amplitudes of Stokes V. In addition, the downflow velocity can be derived from the zero-crossing of Stokes V (this may be considered as step 0).

An important feature of this approach is that we use the Stokes Q profile not only to determine the inclination of the field, but also as the main temperature diagnostic and as an additional constraint on the magnetic field strength. This strong involvement of Stokes Q is one of the major differences between our procedure and others used in the past to determine fluxtube properties from few lines (e.g. Harvey et al., 1972; Frazier and Stenflo, 1978; Koutchmy and Stellmacher, 1978). Also, by using this combination of diagnostic techniques in the given order, we try to reduce the number of uncertainties and assumptions to a minimum, thus coming a step closer to the ideal of a completely self-consistent procedure.

The data we shall use in the second half of the paper have been described by Stenflo et al. (1987a), henceforth called Paper I, who have also carried out a preliminary qualitative analysis not involving radiative transfer calculations. The present paper can therefore also be seen as a quantitative extension of Paper I. Since the zero-crossing wavelengths and asymmetries of the Stokes V profiles of Fe I 5250.2 Å and Fe I 5247.1 Å have already been determined and exhaustively discussed there, we need not consider these parameters further here.

2. Basic considerations and numerical experiments

2.1. Stokes Q asymmetry and the I_Q, I_U, and I_V profiles for saturated lines

Broad-band linear polarization in active regions and sunspots was discovered by Dollfus (1958). Leroy (1962) extended these observations and presented a first interpretation. Using Unno's (1956) solution for Stokes Q he demonstrated that the area of the π-component is different from the summed area of the σ-components of a spectral line with a certain amount of saturation. This saturation effect is often called magnetic intensification. Since Stokes Q and U are identical, except for their different dependences on the azimuth χ, it is sufficient to demonstrate this result for Stokes Q. Calamai et al. (1975) extended his interpretation to include magnetooptical effects by using Rachkovsky's (1967) solution instead of Unno theory.

However, the discussion of broadband polarization fails to make clear that the σ-π asymmetry of Stokes Q persists even for small field strengths, B, since the integrated quantity which is important for broadband linear polarization

$$\int Q\, d\lambda \to 0 \quad \text{for } B \to 0, \tag{1}$$

i.e. the absolute σ-π asymmetry disappears for small magnetic field strengths. However, the relative asymmetry, defined as

$$\delta Q = \frac{A_{\sigma_b} + A_{\sigma_r} - A_\pi}{A_{\sigma_b} + A_{\sigma_r} + A_\pi} = \frac{\int Q\, d\lambda}{\int |Q|\, d\lambda}, \tag{2}$$

does not disappear, as the following Milne-Eddington calculations demonstrate. In Eq. (2) A_{σ_b} is the absolute area of the blue wing (σ-component) of Stokes Q, A_{σ_r} the area of its red wing, and A_π the absolute area of its central or π-component. Note that in certain cases the Q profile may have no π component (for an example see Fig. 3). Then A_π is zero and $\delta Q = 1$.

The relative Q asymmetry has the advantage that it is independent of the amount of flux (it may, however, be affected indirectly if fluxtube properties are a function of the amount of flux), and has a higher diagnostic potential than the absolute asymmetry. Furthermore, with the availability of spectrally resolved observations of Stokes Q (cf. Paper I), its determination is no longer a problem. Since it behaves quite differently from the absolute asymmetry we shall examine it in some detail. In particular, we demonstrate that its existence implies that the relation

$$Q \approx -\frac{1}{4}\Delta\lambda_H^2 \frac{d^2 I}{d\lambda^2}, \tag{3}$$

derived by Stenflo (1985) for a weak magnetic field perpendicular to the line of sight, is in general not valid.

We make use of the solution of Unno (1956). The expressions for the Stokes profiles normalised to the local continuum then read

$$\begin{aligned}
I(\mu) &= \frac{\beta_0\mu}{1+\beta_0\mu}\left(1 - \frac{1+\eta_I}{(1+\eta_I)^2 - \eta_Q^2 - \eta_U^2 - \eta_V^2}\right),\\
Q(\mu) &= \frac{\beta_0\mu}{1+\beta_0\mu}\,\frac{\eta_Q}{(1+\eta_I)^2 - \eta_Q^2 - \eta_U^2 - \eta_V^2},\\
U(\mu) &= \frac{\beta_0\mu}{1+\beta_0\mu}\,\frac{\eta_U}{(1+\eta_I)^2 - \eta_Q^2 - \eta_U^2 - \eta_V^2},\\
V(\mu) &= \frac{\beta_0\mu}{1+\beta_0\mu}\,\frac{\eta_V}{(1+\eta_I)^2 - \eta_Q^2 - \eta_U^2 - \eta_V^2},
\end{aligned} \tag{4}$$

where $\mu = \cos\theta$, β_0 is proportional to the gradient of the Planck function, assumed to be linear in $\tau[B_\nu = B_{\nu_0}(1 + \beta_0\tau)]$, and

$$\begin{aligned}
\eta_I &= \frac{\eta_0}{2}\sin^2\gamma + \frac{\eta_+ + \eta_-}{4}(1 + \cos^2\gamma),\\
\eta_Q &= \left(\frac{\eta_0}{2} - \frac{\eta_+ + \eta_-}{4}\right)\sin^2\gamma\cos 2\chi,\\
\eta_U &= \left(\frac{\eta_0}{2} - \frac{\eta_+ + \eta_-}{4}\right)\sin^2\gamma\sin 2\chi,\\
\eta_V &= \frac{\eta_- - \eta_+}{2}\cos\gamma.
\end{aligned} \tag{5}$$

η_0, η_+, and η_- are the absorption coefficients for the transitions with $\Delta M = 0, \pm 1$. In general they have the spectral shape of a Voigt function, which may be shifted due to Zeeman splitting.

We have neglected magnetooptical effects since they are very small for the weak field case which we shall consider next.

However, they are included in the numerical radiative transfer calculations presented in Sect. 2.2. The simple Milne-Eddington calculations mainly serve to enhance our basic understanding, since the radiative transfer calculations alone, although providing a more general result, are not particularly transparent. In a weak magnetic field (or to be more precise when the Zeeman splitting is small compared to the Doppler width of the line) Eq. (4) simplifies to

$$\begin{aligned} I &= \frac{\beta_0\mu}{1+\beta_0\mu}\left(1-\frac{1}{1+\eta_0}\right), \\ Q &= \frac{\beta_0\mu}{1+\beta_0\mu}\frac{\eta_Q}{(1+\eta_0)^2}, \\ U &= \frac{\beta_0\mu}{1+\beta_0\mu}\frac{\eta_U}{(1+\eta_0)^2}, \\ V &= \frac{\beta_0\mu}{1+\beta_0\mu}\frac{\eta_V}{(1+\eta_0)^2}. \end{aligned} \tag{6}$$

Note that in this approximation the expression for I is identical to the expression in the absence of a magnetic field. Mathys and Stenflo (1987) have derived a relation between η_Q and η_0, which, for a Zeeman triplet in a weak magnetic field, can be written as

$$\eta_Q \approx -\frac{1}{4}\sin^2\gamma\cos 2\chi\,\Delta\lambda_H^2\frac{d^2\eta_0(\lambda)}{d\lambda^2}, \tag{7}$$

so that we obtain

$$Q \approx -\frac{1}{4}\frac{\beta_0\mu}{1+\beta_0\mu}\frac{\sin^2\gamma\cos 2\chi\,\Delta\lambda_H^2}{(1+\eta_0(\lambda))^2}\frac{d^2\eta_0(\lambda)}{d\lambda^2}. \tag{8}$$

In Eqs. (7) and (8) $\Delta\lambda_H$ is the Zeeman splitting

$$\Delta\lambda_H = 4.67\,10^{-13}\,gB\lambda^2, \tag{9}$$

where B is in G and λ in Å.

Since $\eta_0(\lambda)$ has the form of a Voigt function centred on the line, the denominator is larger for line centre, which reduces the area of the π component, leading to the observed asymmetry. In order to obtain a relation between $d^2I/d\lambda^2$ and Q we take the second derivative of the weak field Unno solution of Stokes I

$$\frac{d^2I}{d\lambda^2} \approx -\frac{\beta_0\mu}{1+\beta_0\mu}\left(\frac{2}{(1+\eta_0(\lambda))^3}\left(\frac{d\eta_0(\lambda)}{d\lambda}\right)^2 - \frac{1}{(1+\eta_0(\lambda))^2}\frac{d^2\eta_0(\lambda)}{d\lambda^2}\right). \tag{10}$$

If we use Eq. (10) to replace $d^2\eta_0(\lambda)/d\lambda^2$ in Eq. (8), then we get not only a $d^2I/d\lambda^2$ term, but also a $(d\eta_0/d\lambda)^2$ term. This has the effect that the relative asymmetry of Q does not disappear even for very small fields. It is only for very weak (i.e. unsaturated) lines with $\eta_0(\lambda) \to 0\,\forall\lambda$ that we regain the relationship [Eq. (3)] derived by Stenflo (1985).

Let us, for the moment, turn to Stokes V. Since the two σ-components are completely equivalent with respect to saturation in a static atmosphere, the Stokes V profile fortunately suffers no similar consequences. This can be shown very simply by combining Eq. (6) with the relation (e.g. Mathys and Stenflo, 1987)

$$\eta_V \approx -\cos\gamma\,\Delta\lambda_H\frac{\partial}{\partial\lambda}\eta_0(\lambda). \tag{11}$$

The resulting relation between Stokes V and I reads (including line saturation)

$$V = -\cos\gamma\Delta\lambda_H\frac{dI}{d\lambda}. \tag{12}$$

Therefore, this relation, which was derived by Stenflo et al. (1984) without regard for saturation effects, is valid for lines of all strengths, as long as the Zeeman splitting is sufficiently small.

The above results are of consequence for the so called I_V, I_Q, and I_U profiles, the first of which was introduced by Solanki and Stenflo (1984). For Zeeman triplets these profiles can be defined as (neglecting an additive constant and a factor resulting from the finite filling factor and continuum contrast of the fluxtubes)

$$I_V = -\frac{1}{\cos\gamma\,\Delta\lambda_H}\int_{\lambda_1}^{\lambda} V(\lambda')\,d\lambda', \tag{13}$$

$$I_Q = -\frac{4}{\sin^2\gamma\cos 2\chi\,\Delta\lambda_H^2}\int_{\lambda_1}^{\lambda} d\lambda'\int_{\lambda_1'}^{\lambda'} d\lambda''\,Q(\lambda''), \tag{14}$$

$$I_U = -\frac{4}{\sin^2\gamma\sin 2\chi\,\Delta\lambda_H^2}\int_{\lambda_1}^{\lambda} d\lambda'\int_{\lambda_1'}^{\lambda'} d\lambda''\,U(\lambda''). \tag{15}$$

For anomalously split lines analogous expressions can be derived using the expansion technique of Mathys and Stenflo (1987) (cf. Solanki, 1987b). In Eqs. (13), (14), and (15) λ_1 and λ_1' are wavelengths far enough in the blue wings of the lines for the polarized profiles to approach zero. A comparison of Eq. (13) with Eq. (12) shows that the I_V profile is an approximation of the Zeeman unsplit Stokes I in the magnetic region, and since Eq. (12) is valid for *all* lines in a sufficiently weak field, this interpretation of the I_V profile will also be valid for all lines. On the other hand the I_Q profile is an approximation of the unsplit Stokes I only for very weak lines, since the differential form of this equation, Eq. (3), is only valid for very weak lines. For stronger lines the presence of the Stokes Q σ-π asymmetry means that I_Q will not be even faintly similar to Stokes I and is, therefore, of no practical value, especially if $A_{\sigma_b} + A_{\sigma_r} > 2A_\pi$, which is the case for all profiles with $\delta Q > \frac{1}{3}$. An example of such a Q profile is illustrated in Fig. 3 (the narrowest profile, solid curve). More will be said to this figure in Sect. 2.2. The same is also true for the I_U profile. Furthermore, it can be easily shown that other possible definitions of I_Q and I_U, which try to incorporate the asymmetry, e.g. via a combination of Eqs. (8) and (10), require the solution of a non-linear differential equation. This is obviously unfeasible.

2.2. *Dependence of Q asymmetry on various parameters*

In this section we investigate the dependence of δQ on magnetic field strength B, oscillator strength $\log gf$, angle γ, macroturbulence $\xi_{\rm mac}$, microturbulence $\xi_{\rm mic}$, and temperature T. One respect in which these calculations differ from those of Leroy (1962), Calamai et al. (1975), and Landi Degl'Innocenti and Calamai (1982) is that we use a proper radiative transfer code and apply it to a real line in the solar spectrum. Previous authors used only the simple Milne-Eddington theories of Unno (1956) or Rachkovsky (1967). However, the main difference is that we examine the *relative* asymmetry of Q whose properties can be quite different from those of the absolute asymmetry which has previously been exclusively investigated.

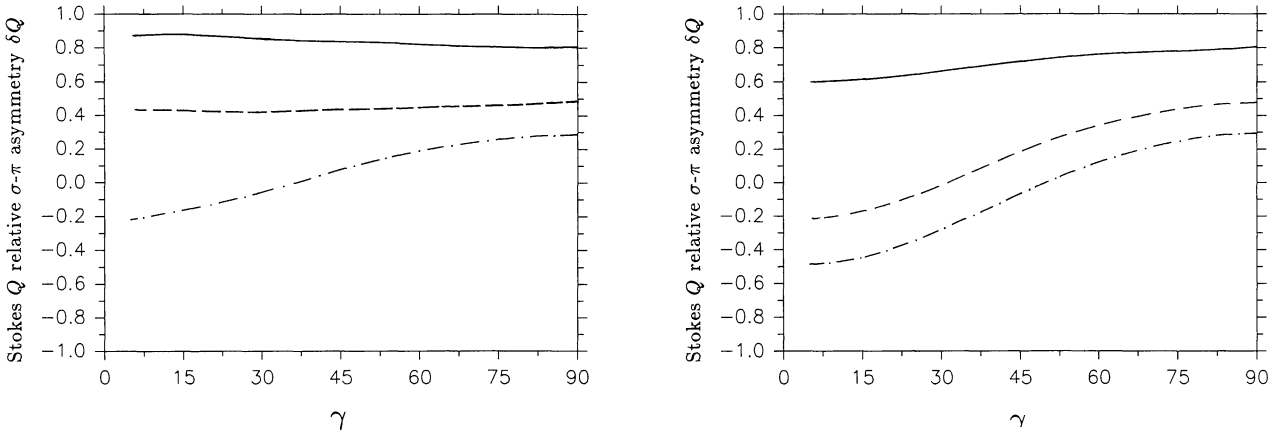

Fig. 1. The relative Q area asymmetry, δQ, as a function of γ, the angle between the magnetic field and the line of sight for the Fe I 5250.2 Å line calculated in the HSRA at $\mu = 1$. Solid curves: $B = 500$ G, dashed curves: $B = 1000$ G, dot-dashed curves: $B = 1500$ G. *a* Including magnetooptical effects. *b* With magnetooptical effects switched off

The radiative transfer calculations are carried out with the modified code of Beckers (1969a,b), see also Solanki (1987b, Chapter 2). For the trial calculations we generally use a slightly modified version of the HSRA (Gingerich et al., 1971), always assume a constant magnetic field, and usually restrict ourselves to the Fe I 5250.2 Å line.

No dependence of δQ on the azimuth χ is found, while in Fig. 1a the dependence on γ and on field strength is illustrated. The solid curve represents $B = 500$ G, the dashed curve $B = 1000$ G, and the dot-dashed curve $B = 1500$ G. All calculations have been carried out at disk centre with a microturbulence $\xi_{\rm mic} = 0.8\,{\rm km\,s^{-1}}$ and $\xi_{\rm mac} = 0.0$.

The dependence on γ is very small for $B = 500$ and 1000 G, but quite significant for 1500 G. For this field strength the asymmetry actually becomes negative for $\gamma \lesssim 35°$, i.e. the π-component then has a larger area than the two σ-components together. If we keep in mind that the magnetic field in fluxtubes is of the order of 1000–1200 G when assuming a constant field (cf. Sect. 3.3) then we see that this parameter (the Q asymmetry) can be considered to be practically independent of γ. This is particularly true for lines with smaller Landé factors, since a line with, say, $g = 1.5$ in a 1000 G field behaves identically to a line with $g = 3$ in a 500 G field. The γ dependence of δQ at other values of μ is slightly larger, but is never significant for $B = 1000$ G. δQ is also a weak function of θ alone (i.e. with γ fixed). The strong dependence on magnetic field strength is also evident from the figure. Note that δQ *increases* for decreasing field strength, which is of course contrary to the behaviour of the absolute asymmetry.

Fig. 1b illustrates the asymmetry calculated with the magnetooptical effects switched off. As expected, the curves with and without magnetooptical effects coincide for $\gamma = 90°$, and the influence of magnetooptical effects is larger for 1000 G than for 500 G. However, the influence of magnetooptical effects on δQ decreases again above $B = 1000$ G, so that for large field strengths, e.g. $B = 5000$ G, the curves with and without magnetooptical effects practically overlap (not plotted).

For the case without magnetooptical effects one can easily understand the decrease in Q asymmetry with decreasing γ (and even the reversal in the asymmetry). It is due to the decreasing strength of the π-component relative to the total σ-components (and not only the linearly polarized part of them). This means that for small γ the π-component is no longer so strongly saturated and may even become less saturated than the σ-components. This effect becomes more and more important as the field strength increases, which in the Milne-Eddington model corresponds to the increasing strength of the η_Q^2, η_U^2, and η_V^2 terms in the denominators of Eq. (4).

The influence on two additional parameters is illustrated in Fig. 2. There δQ is plotted vs. the macroturbulence velocity $\xi_{\rm mac}$ for lines with different $\log gf$ values. Realistic values of $\xi_{\rm mac}$ in fluxtubes lie in the range $1–3\,{\rm km\,s^{-1}}$ (Solanki, 1986). The calculations underlying the figure have been carried out for $\mu = 1$, $B = 1000$ G, $\xi_{\rm mic} = 0.8\,{\rm km\,s^{-1}}$, and $\gamma = 90°$. Fe I 5250.2 Å with the following $\log gf$ values has been calculated: -3.938 (solid curve), -4.938 (dashed curve, nominal value), and -5.938 (dot-dashed curve). As expected the asymmetry is very strongly dependent on $\log gf$ and therefore the amount of saturation, with the strongest line showing the largest asymmetry. However, the main aim of this figure is to show the strong influence of the macroturbulence which induces an increase in δQ. $\delta Q = 1$ is the maximum defined value of the asymmetry, a limit set by the

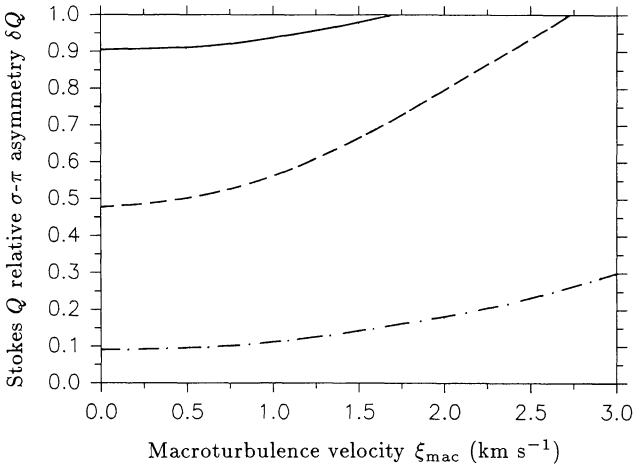

Fig. 2. δQ vs. $\xi_{\rm mac}$, the macroturbulence velocity. HSRA at $\mu = 1$, with $B = 1000$ G and $\gamma = 90°$. Solid curve: $\log gf = -3.938$, dashed curve: $\log gf = -4.938$ (Fe I 5250.2 Å line), dot-dashed curve: $\log gf = -5.938$

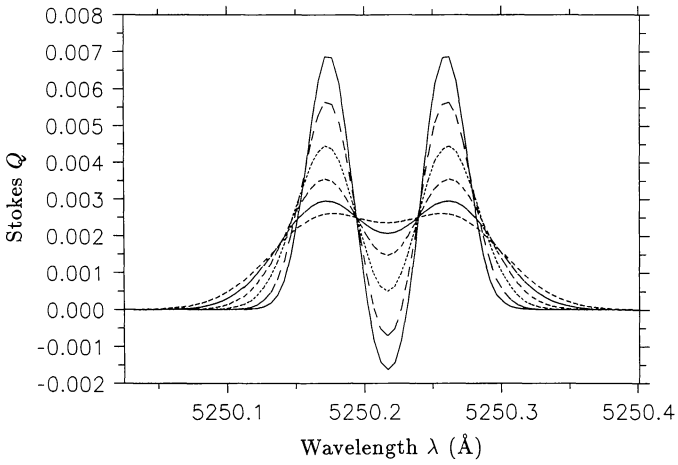

Fig. 3. Stokes Q profiles of Fe I 5250.2 Å with different amounts of macroturbulence broadening. The narrowest profile is unbroadened. The successively broader profiles have been convoluted with $\xi_{mac} = 0.5$, 1.0, 1.5, 2.0, and 2.5 km s^{-1}. Note the disappearance of the π-component with increasing ξ_{mac}

disappearance of the π-component. The influence of ξ_{mac} on Q profiles with $\delta Q < 0$ has also been investigated. We find that $|\delta Q|$ increases with ξ_{mac} in every case, a result which can also be demonstrated analytically.

It is quite instructive to consider in greater detail the influence of a macroturbulence velocity on a Q profile with a large initial δQ. This is illustrated in Fig. 3. The narrowest profile (solid line) is the originally calculated one. Each successively broader profile has been convoluted by a Gaussian macroturbulence with 'Doppler' widths of 0.5, 1.0, 1.5, 2.0, and 2.5 km s^{-1}, respectively. The last four profiles have no π-components at all left, so that their asymmetry cannot be defined. The most broadened profiles look as if they were the result of magnetooptical effects only. This illustrates the danger of interpreting the Q profile shape without taking velocity broadening into account. We have also tested the dependence on microturbulence and find that, for reasonable values of ξ_{mic} (i.e. $\xi_{mic} \leq 2.0$ km s^{-1}), it does not affect δQ very strongly.

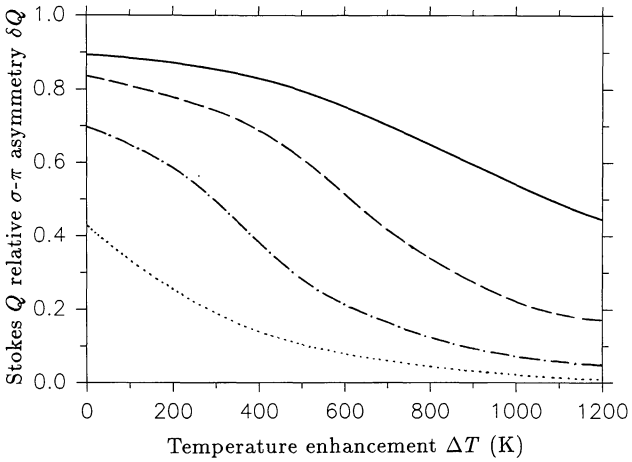

Fig. 4. δQ vs. ΔT, the temperature excess compared to the HSRA. We have chosen $B = 1000$ G, and $\theta = \gamma = 75°$. Solid curve: $\log gf = -3.938$, dashed curve: $\log gf = -4.438$, dot-dashed curve: $\log gf = -4.938$, dotted curve: $\log gf = -5.438$

It should also be noted that since instrumental spectral smearing acts very similarly to macroturbulence broadening, observations with low spectral resolution will also tend to give too large $|\delta Q|$ values. Although the absolute asymmetry ΔQ is independent of both spectral smearing and macroturbulence broadening, it is so strongly dependent on field strength, filling factor, continuum contrast, and γ that it is of only limited use as a fluxtube diagnostic.

A comparison of the profiles calculated with the HSRA to observed Stokes Q profiles has shown that the calculated profiles generally have a much too large asymmetry. This has led to the idea that it could be the higher temperature in the fluxtubes which is responsible for this difference. We have tested this hypothesis, initially by checking the general dependence of δQ on ΔT, later by comparison with the data (Sect. 3.4). We define ΔT as the temperature difference between a particular model atmosphere and the HSRA. The models employed in this section have temperature stratifications parallel to that of the HSRA in the photosphere, so that their $T(\tau)$ can be characterised by a single parameter ΔT.

Figure 4 illustrates the dependence of δQ on ΔT. The other parameters are: $B = 1000$ G, $\gamma = \theta = 75°$, $g = 3$. The four curves correspond to lines with different $\log gf$ values. Each line is sensitive to a certain ΔT range. Thus the line with $\log gf = -5.438$ (dotted curve) is sensitive to $0\,\text{K} \lesssim \Delta T \lesssim 400\,\text{K}$, the line with $\log gf = -4.938$ (dot-dashed curve) to $200\,\text{K} \lesssim \Delta T \lesssim 800\,\text{K}$, the line with $\log gf = -4.438$ (dashed curve) to $400\,\text{K} \lesssim \Delta T \lesssim 1000\,\text{K}$, the line with $\log gf = -3.938$ (solid curve) to $600\,\text{K} \lesssim \Delta T$. The sensitivity (i.e. the gradient of a curve) also depends on Landé factor. Thus Fe I 5247.1 Å is sensitive to almost the same ΔT range as Fe I 5250.2 Å, but its δQ has a stronger gradient there. The excitation potential of the chosen lines also plays a role. Finally, we wish to point out that δQ should also be useful for determining the temperature in sunspot umbrae and penumbrae. However, totally different lines are required for their study.

2.3. *Numerical experiments with the Q/V ratio*

We have tested the dependence of the Q/V ratio on γ, χ, θ, B, ξ_{mic}, ξ_{mac}, and ΔT. Two different parameters have been used, one based on the amplitudes of the σ-components

$$\frac{Q}{V}(a) = \frac{a_\sigma(Q)}{a_\sigma(V)} \frac{\cos\gamma}{\sin^2\gamma}, \tag{16}$$

the other on their areas, $Q/V(A)$, which is defined similarly. In Eq. (16) $a_\sigma(Q)$ is the sum of the amplitudes of the blue and the red σ components of the Stokes Q profile, while $a_\sigma(V)$ is the sum of the blue and red Stokes V amplitudes. The factor $\cos\gamma/\sin^2\gamma$ is the γ dependence of η_V/η_Q, so that $Q/V(A)$ and $Q/V(a)$ are to first order independent of γ, although a small γ influence may be induced by radiative transfer effects. These definitions of Q/V are ideal for testing the influence of parameters other than γ on Q/V. Our calculations show that the parameters with the largest influence on $Q/V(a)$ and $Q/V(A)$ are B and ξ_{mac}. The influence of B has been pointed out earlier by Stenflo (1985) on the basis of Milne-Eddington calculations. Our numerical calculations confirm his result that γ will be overestimated if the filamentary nature of the magnetic field is not taken into account. For observations near disk centre this means that the fields will appear more horizontal than they actually are. However, if we have a

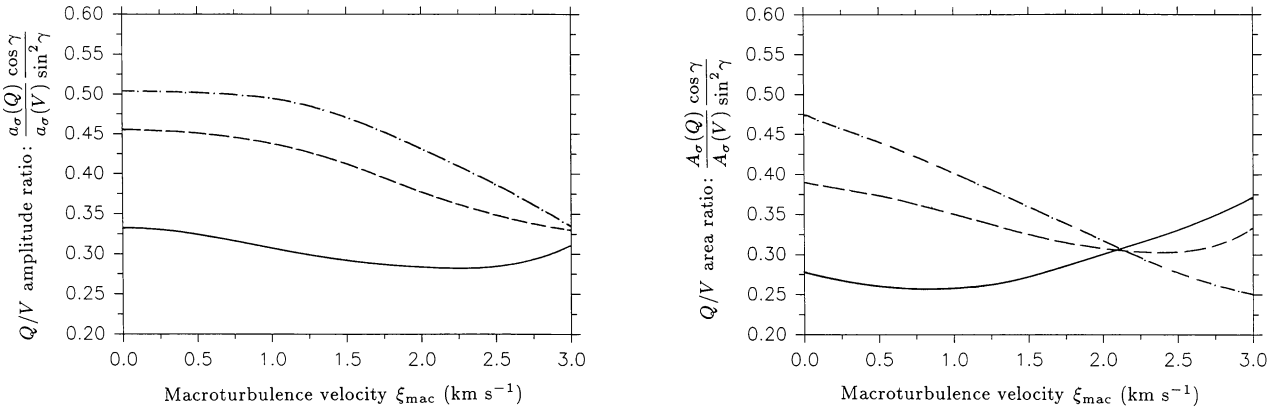

Fig. 5. Q/V ratio vs. ξ_{mac} for Fe I 5250.2 Å in the HSRA with $\mu = 1$ and $\gamma = 45°$. Solid curve: $B = 500$ G, dashed curve: $B = 1000$ G, dot-dashed curve: $B = 1500$ G. **a** $Q/V(a)$, the ratio of the amplitudes of the Q σ-components to the V σ-components. **b** $Q/V(A)$, the ratio of the areas

rough idea of B (within ± 300 G) and ξ_{mac} (within ± 0.5 km s^{-1}) in the fluxtube, we should be able to reduce their combined influence on γ to less than 5°.

The dependence of $Q/V(a)$ and $Q/V(A)$ on ξ_{mac} and B is illustrated in Fig. 5. The solid curves represent $B = 500$ G, the dashed curves $B = 1000$ G, and the dot-dashed curves $B = 1500$ G. Due to their narrowness, the σ-components of Stokes Q are initially affected more strongly than the σ-components of V. This leads to a decrease in Q/V with ξ_{mac}, which may reverse into an increase after the π-component has disappeared (which happens first for $Q/V(A)$ of $B = 500$ G, cf. Fig. 2). Besides having a somewhat smaller dependence on ξ_{mac} than $Q/V(A)$, $Q/V(a)$ is also less sensitive to temperature (its temperature sensitivity is minute, γ changes by less than 3° when T changes by 1200 K) and to θ. We shall therefore use the amplitudes when comparing with the data. Note that the influence of a lower spectral resolution on the observed Q/V is similar to the influence of a larger ξ_{mac} on the calculated ratio. The influence of spectral smearing on Stokes V alone has been discussed by Solanki and Stenflo (1986).

2.4. Numerical experiments with the 5250/5247 Stokes V and Q line ratios

The influence of various parameters on the Stokes V (and partly also Stokes Q) line ratio of Fe I 5250.2 Å to Fe I 5247.1 Å has been examined as well. Besides the well known dependence on magnetic field strength, which was first used to diagnose the kilogauss nature of non-sunspot magnetic fields by Stenflo (1973), and a relative insensitivity to temperature and θ we find a surprisingly large dependence on γ and ξ_{mac}. In this section we restrict ourselves to a short discussion on the influence of γ. The ξ_{mac} and temperature dependence will be discussed in Sect. 3.3, when comparing with the data.

In Fig. 6a the 5250/5247 Stokes V line ratio is plotted vs. γ for two different θ values, $\theta = 0°$ (solid line) and $\theta = 75°$ (dashed line). We define the V line ratio as $a_\sigma(V, 5250)/(1.5 \times a_\sigma(V, 5247))$, where 1.5 is the ratio of the effective Landé factors of the two lines. The temperature structure is that of the HSRA with a constant magnetic field of 1000 G. The illustrated dependence on γ

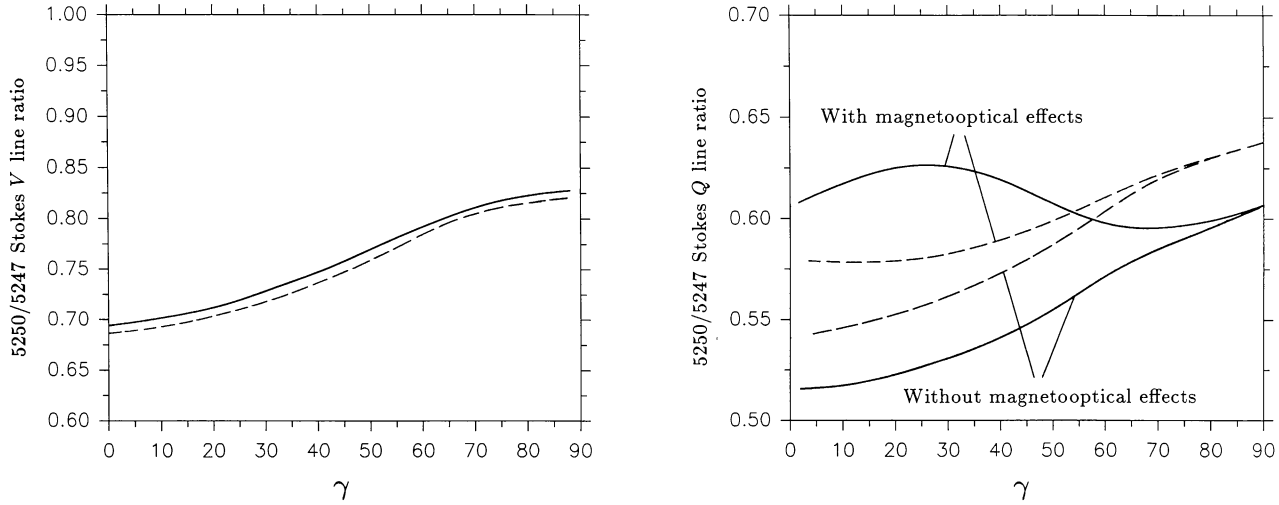

Fig. 6. 5250/5247 line ratio vs. γ for the HSRA with $\mu = 1$, $B = 1000$ G, $\theta = 0°$ (dashed curves) and $\theta = 75°$ (solid curves). a Ratio of the V profiles, defined as $a_\sigma(V, 5250)/(1.5 \times a_\sigma(V, 5247))$, where a_σ is the sum of the blue and red amplitudes. Calculations with and without magnetooptical effects give the same curves. **b** Ratio of the Q profiles, defined as $a_\sigma(Q, 5250)/(2.25 \times a_\sigma(Q, 5247))$. Lower curve for each θ is without magnetooptical effects

can lead to a wrong field strength being determined if γ differs from the value assumed for it.

Since the change in the line ratio with γ (while keeping θ constant) cannot be an effect of changing line width, we must find another explanation. Magnetooptical effects can be ruled out, since calculations with such effects switched off give curves which are identical to the ones plotted. The main remaining effect of varying γ is that the π-component changes in strength relative to the σ-components. Although the Stokes V absorption coefficient involves only the circularly polarized part of the σ-components, the emergent V profile is coupled to the other Stokes parameters via the radiative transfer equations and is sensitive to the π-component as well, in particular for lines with large splitting. The qualitative form of this dependence can be easily verified with the help of Eq. (4) using one strongly split and one weakly split line. The analytical calculations clearly demonstrate that the effect is due to the π-component.

For the Q line ratio, defined as $a_\sigma(Q, 5250)/(2.25 \times a_\sigma(Q, 5247))$, we would theoretically expect (Milne-Eddington model) a similar dependence on γ as Stokes V. The factor 1/2.25 in the definition of the Q line ratio is the ratio of the squared Landé factors of the two lines. The numerical treatment in Fig. 6b (solid and dashed curves correspond to $\theta = 0°$ and 75°, respectively) indeed shows a dependence on γ, quantitatively similar to that exhibited by Stokes V when magnetooptical effects are switched off (the lower curves in Fig. 6b). Whereas the V ratio changes by a factor of 1.19 when going from $\gamma = 5°$ to 85°, the Q line ratio changes by a factor of 1.16. With magnetooptical effects switched on the dependence is considerably reduced (upper curves). The influence of the magnetooptical effects is largest for small γ values on the line ratio, as is the case for the Q asymmetry.

3. Comparison with the data

3.1. Data and models

Let us now apply the procedure outlined in Sect. 1 to the data. We wish to stress that we are only attempting to illustrate the application of this procedure and are not deriving a definitive model of fluxtubes. The data we shall use were obtained in 1979 and 1984 with the 1-m Fourier transform spectrometer (FTS) and the McMath telescope of the National Solar Observatory. Stokes I and V were observed in 1979 and I, V, and Q in 1984. The 1979 data have been discussed by Stenflo et al. (1984) and the 1984 data in Paper I. In the present paper we shall only consider the Fe I 5250.2 Å and Fe I 5247.1 Å lines, and shall concentrate particularly on the centre to limb variation (CLV) of their parameters. These have already been qualitatively analysed in Paper I, so that we can directly adopt many of the representations used there.

Since eight of the ten spectra we use were obtained in active region plages, we shall mostly use the plage model of Solanki (1986). The present calculations therefore consist of the first test of the plage model away from disk centre. The main assumptions underlying this model are: thin fluxtube approximation for the magnetic field, LTE radiative transfer restricted to one line of sight, and a mixture of micro- and macroturbulence to describe the velocity broadening of the lines. The most restrictive assumption is probably the one line of sight radiative transfer (i.e. a plane parallel fluxtube). As Van Ballegooijen (1985a,b) has shown, the geometry of fluxtubes is important for the calculated profiles. However, it is beyond the scope of the present paper to include a 1.5-D radiative transfer.

3.2. Turbulence velocity inside fluxtubes

Solanki (1986) has represented the velocity broadening inside fluxtubes by a mixture of macro- and microturbulence. Due to the simplicity of this approach we shall make use of it here as well. First we model the CLV of the Stokes I profiles of the two lines, this being a good test for the method and the code.

The CLV of the microturbulence, as determined from Fe I lines in the quiet photosphere, has been published by Simmons and Blackwell (1982). The $\xi_{\rm mic}$ values of Simmons and Blackwell increase linearly with decreasing μ, except for their last point at $\mu = 0.2$. For our calculations up to $\mu = 0.1$ we have to extrapolate from their values. Keeping in mind that Simmons and Blackwell feel that the value at $\mu = 0.2$ is less certain than the rest, we have neglected it for our rough analysis and extrapolate linearly from the rest of the points. We therefore adopt the following dependence of $\xi_{\rm mic}$ on μ:

$$\xi_{\rm mic} = -0.69\mu + 1.61\ {\rm km\,s^{-1}} \quad \text{for } 0.1 \le \mu \le 1.0. \tag{17}$$

Values for the macroturbulence in the quiet photosphere for disk centre and near the limb have been listed by Holweger et al. (1978). We interpolate in their data to obtain the linear relation for the macroturbulence

$$\xi_{\rm mac} = -0.78\mu + 2.08\ {\rm km\,s^{-1}} \quad \text{for } 0.1 \le \mu \le 1.0, \tag{18}$$

which we have used to broaden the Stokes I profiles calculated with the HSRA keeping $B = 0$. These are then compared with the data. Since the data were mostly obtained in active regions with sometimes sizeable filling factors (cf. Sect. 3.7), the fits are not quite ideal. In particular the line depths of the observed profiles are smaller than of the calculated ones. However, for Fe I 5247.1 Å the line widths match rather well. For Fe I 5250.2 Å, on the other hand, the magnetic broadening of the I profile is appreciable and the calculated profiles are generally too narrow.

The disk centre analysis of Solanki (1986) has shown that $\xi_{\rm mic}$ cannot be much larger inside fluxtubes than outside them, and that the best fit is obtained when $\xi_{\rm mic}^{\rm Fluxtube} \approx \xi_{\rm mic}^{\rm Photosphere}$. Since it is rather difficult to determine the relative fractions of the macro- and microturbulence from only two lines, we shall assume that $\xi_{\rm mic}^{\rm Fluxtube}(\mu) = \xi_{\rm mic}^{\rm Photosphere}(\mu)$ for all μ.

From a comparison of observed to calculated V profiles, we find values of $\xi_{\rm mac}^{V}$ (i.e. $\xi_{\rm mac}$ determined from Stokes V) between 2.0 and 2.5 km s^{-1}, with no clear dependence on μ visible. The spread in $\xi_{\rm mac}^{V}$ values is mainly due to the uncertainty in its determination. Thus, in contrast to Stokes I, the macroturbulence broadening does not increase towards the limb, but neither does it decrease, as would be expected if the mass motions in fluxtubes were mainly vertical. However, we cannot reach definite conclusions regarding the velocity structure from just these two lines. We also wish to point out that the fits to the observed Stokes V profile shapes are often not of very good quality. This is partly due to the asymmetry of the observed Stokes V, and partly due to the fact that the central portion of the observed V profiles is much flatter than that of the calculated profiles. This is suggestive of the influence of the finite thickness of the fluxtube (Solanki and De Martino, in preparation).

It is heartening that the $\xi_{\rm mac}^{V}$ values at $\mu \approx 1$ determined by directly fitting the V profiles of these lines are similar to those

determined from their I_V profiles by Solanki (1986), who found $\xi^V_{\rm mac} = 1.9\,{\rm km\,s^{-1}}$ for both lines, while we obtain $2.0\,{\rm km\,s^{-1}}$. Note that we have been unable to reproduce the shapes of the V profiles of 5247.1 Å and 5250.2 Å simultaneously without a strong magnetic field. Therefore, more will be said about the velocity broadening after determining the field strength in the next section.

3.3. Centre-to-limb variation of the Stokes V and Q5250/5247 line ratios

Next we compare calculations of the Stokes V and Q 5250/5247 line ratios with the data (cf. Fig. 2 of Paper I). We have not made use of the regression equation for the CLV of the V line ratio introduced in that paper due to the problems mentioned there. The V ratio has been previously calculated by a number of authors (e.g. Stenflo, 1973, 1975; Frazier and Stenflo, 1978; Wiehr, 1978; Stenflo and Harvey, 1985; Semel, 1986). However, the calculations presented here contain some improvements and additions compared to most previous determinations. Firstly, we calculate the line profiles numerically. With the exception of Stenflo (1975) and Wiehr (1978) previous investigators have used the Milne-Eddington solutions of Unno or Rachkovsky. Secondly, we calculate the CLV of the line ratio. Thirdly, we use both a model with constant field and one based on the thin fluxtube approximation, i.e. with a magnetic field whose strength decreases rapidly with height. Fourthly, we test for the sensitivity of the line ratio to temperature by calculating it for both the HSRA and the plage fluxtube model. Fifthly, we also include the influence of macroturbulence broadening on the line ratio.

Figure 7a shows the measured CLV of the Stokes V 5250/5247 line ratio, as well as model calculations involving the plage model with a magnetic field calculated using the thin tube approximation. The magnetic field vector is assumed to be vertical to the solar surface, i.e. $\cos\gamma = \mu$. For the microturbulence we make use of Eq. (17). The solid curves represent the line ratio of the profiles unbroadened by macroturbulence. For the upper solid curve the magnetic field strength at $\tau = 1$, $B(\tau = 1) = 1400\,{\rm G}$, for the lower solid curve $B(\tau = 1) = 2000\,{\rm G}$.

The solid curves in Fig. 7a give the impression that the 1400 G model provides the better fit to the data. However, a comparison of the complete calculated Stokes V profiles with the observations clearly shows that the former are much too narrow, in agreement with the conclusions of Sect. 3.2. After broadening with an appropriate macroturbulence we obtain the dashed curves in Fig. 7a. Now it is the model with the higher field strength which gives the better fit. This large influence of velocity broadening on the line ratio is also mirrored in the large influence of spectral smearing on this parameter (Solanki, 1987b).

With the scatter the $B(\tau = 1) = 2000\,{\rm G}$ model fits the data quite well and suggests that the thin tube approximation is a reasonable assumption. But, before concluding anything on the height dependence of the magnetic field, let us first test this diagram for its sensitivity to magnetic field gradients. We have therefore also calculated profiles for a series of models with constant magnetic fields. The resulting 5250/5247 line ratio vs. μ curve of one such model ($B = 1140\,{\rm G} = {\rm constant}$) is plotted in Fig. 7b (dashed curve) together with that of the thin tube model with $B(\tau = 1) = 2000\,{\rm G}$ (solid curve). The two models give identical results for $\mu = 1$, and diverge slightly near the limb. Their difference is, however, considerably smaller than the scatter in the data. We therefore conclude that it is presently not possible to determine the height variation of the magnetic field from the CLV of the line ratio with one-dimensional models.

There are two possible explanations for this insensitivity to the magnetic field gradient. The first is that it is the change in line shape which dominates the CLV of the line ratio. The increasing width of the lines near the limb simulates the presence of a weaker field (cf. Paper I and Stenflo et al., 1987b) and the increasing relative strength of the π-component with increasing γ also contributes to the change in the line ratio (cf. Sect. 2.4). Another possibility is that inside fluxtubes the lines are formed at nearly the same height near the limb as at disk centre. Calculations of the heights of formation in fluxtubes are of great importance to settle this question.

This result is in contrast to the findings of Stenflo et al. (1987b), who used a simple model of the Zeeman splitting of these lines

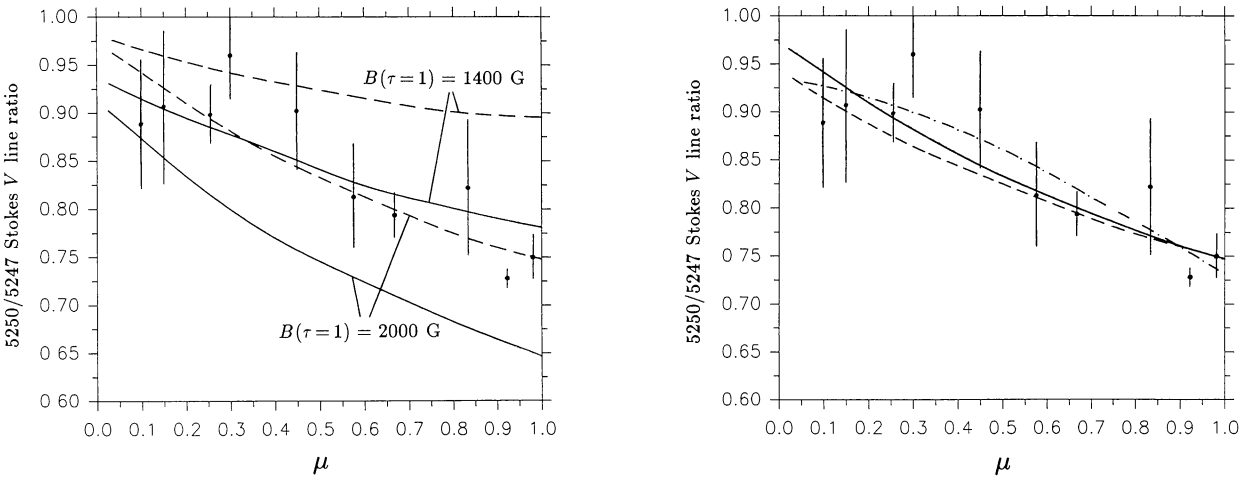

Fig. 7. 5250/5247 Stokes V amplitude line ratio vs. μ. Filled circles are FTS data, the curves model calculations. **a** Line ratio calculated using a plage model and the thin tube approximation with $B(\tau = 1) = 2000\,{\rm G}$ and 1400 G, respectively, as marked in the figure. Solid curves: $\xi_{\rm mac} = 0$, dashed curves: $\xi_{\rm mac} \approx 2.0\,{\rm km\,s^{-1}}$. **b** Solid curve: Plage model and the thin tube approximation with $B(\tau = 1) = 2000\,{\rm G}$. Dashed curve: Plage model and a constant magnetic field of strength 1140 G. Dot-dashed curve: HSRA, $B = 1300\,{\rm G} = {\rm constant}$

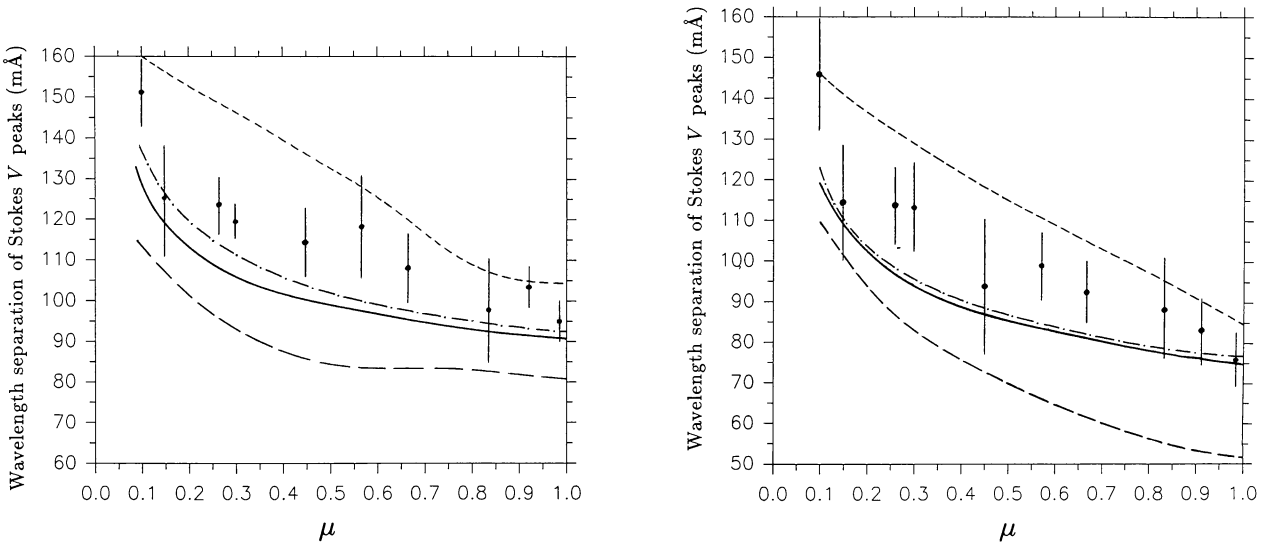

Fig. 8. V peak separation vs. μ. Filled circles: FTS data. Solid curves: Plage model with thin tube magnetic field having $B(\tau = 1) = 2000\,\mathrm{G}$, $\xi_{\mathrm{mac}} \approx 2.0\,\mathrm{km\,s^{-1}}$. Dot-dashed curves: Plage model with $B = 1140\,\mathrm{G}$ = constant and $\xi_{\mathrm{mac}} \approx 2.0\,\mathrm{km\,s^{-1}}$. Short dashes: HSRA with $B = 1300\,\mathrm{G}$ = constant and $\xi_{\mathrm{mac}} = 1.7\,\mathrm{km\,s^{-1}}$. Long dashes: Plage model with $B = 1140\,\mathrm{G}$ = constant and $\xi_{\mathrm{mac}} = 0.0\,\mathrm{km\,s^{-1}}$. **a** Fe I 5250.2 Å. **b** Fe I 5247.1 Å

to infer a considerable decrease in field strength with decreasing μ. Although the model of Stenflo et al. (1987b) takes into account the increase in line width, it makes no provision for the increasing importance of the π-component near the limb. This is the main reason for its difference to the radiative transfer calculations presented here.

The dot-dashed curve in Fig. 7b is the CLV of the line ratio calculated with the HSRA and $B = 1300\,\mathrm{G}$ = const. The difference to the other two curves is again less than the scatter in the data. We conclude that, as expected, the line ratio is rather insensitive to the temperature.

The importance of the macroturbulent broadening can also be judged from Fig. 8 (Fig. 8a: Fe I 5250.2 Å, Fig. 8b: 52471.1 Å). There the wavelength separation of the blue and red peaks of Stokes V is plotted as a function of μ, both for the data (cf. Fig. 3a of Paper I) and some models which reproduce the V line ratio. The best fits to the data are given by the plage atmosphere thin tube $B(\tau = 1) = 2000\,\mathrm{G}$ (solid) and $B = 1140\,\mathrm{G}$ = constant (dot-dashed) models including macroturbulence broadening. The unbroaden $B(\tau = 1) = 1400\,\mathrm{G}$ thin tube model (long dashes) and the HSRA $B = 1300$ = constant model (short dashes) reproduce this line parameter rather badly. For the HSRA this is due to the fact that we cannot reproduce the CLV of the line ratio and of the line widths simultaneously, and we have opted to reproduce the line ratio.

The fact that even the macro-broadened profiles calculated with the plage model cannot reproduce this diagram properly has to do with the different line shapes of observed and calculated profiles. Since we have always tried to fit the *complete* profile as well as possible, the peak wavelength separation could not always be fitted to the desired accuracy. The residual difference between observed and calculated profiles stems partly from the asymmetry between the blue and red wings of the observed V profiles, but it may also have to do with the fact that our models are restricted to one line of sight. This is particularly true for the data away from disk centre.

In Fig. 8 both lines are reproduced almost equally well by the broadened plage models. Since we have always broadened both lines with the same velocity, this observation supports the magnetic field strength deduced from the V line ratio. We have also tried to match the peak separation line ratio (introduced in Paper I), but have found that none of the models give a reasonable fit, in agreement with Stenflo et al. (1987b), who also could not reproduce the amplitude and the peak separation line ratios simultaneously.

A further check on the field strength is provided by the 5250/5247 Q line ratio, which is plotted vs. μ in Fig. 9. The data are taken from Fig. 2 of Paper I, while the models are the same as in Fig. 7b. This diagram is also not sensitive to the height gradient of the magnetic field. Note that the CLV of the Q ratio is considerably smaller than for V, as expected from Fig. 6. The Q profiles have been broadened with the same velocity as the V profiles. The fit to the data is reasonable, which is not too surprising since the error bars are rather large. For the Stokes Q line ratio, the HSRA with 1170 G (not plotted) gives a curve

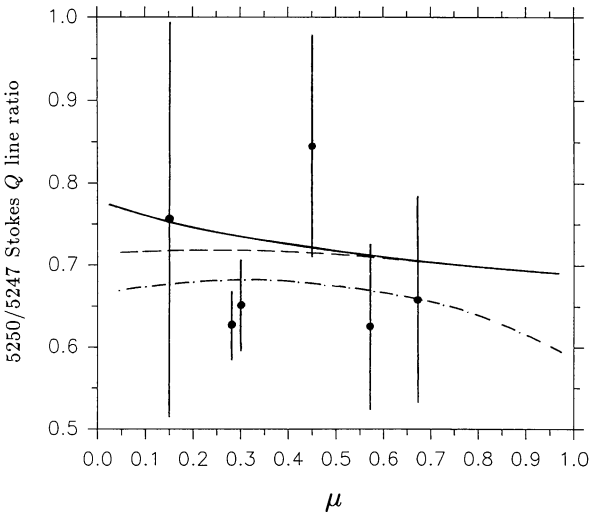

Fig. 9. 5250/5247 Stokes Q line ratio vs. μ. The models are the same as in Fig. 7b

which lies closer to the other models than the HSRA with 1300 G. Hopefully, future observations of Stokes Q with better signal to noise ratios will provide more stringent constraints on the field strength.

3.4. Q asymmetry and temperature

The calculations of Sect. 2.2 have shown that the Q asymmetry, δQ, is influenced mostly by magnetic field strength, turbulence velocity, and temperature. In Sects. 3.2 and 3.3 we have determined the velocity broadening and the magnetic field strength from the Stokes V profile, so that we can now use δQ to set constraints on fluxtube temperature.

The CLV of δQ of the observed and calculated profiles is plotted in Figs. 10a and b for Fe I 5250.2 Å and 5247.1 Å, respectively. The plotted curves belong to the same models as in Fig. 7b. The synthetic Stokes Q profiles have been broadened by the same velocity as Stokes V. The plage temperature model reproduces δQ considerably better than the HSRA, although for $\mu < 0.2$ the HSRA appears to be marginally better. If this is due to a true decrease in temperature with height or has another origin, cannot be decided at present. In both diagrams the plage model with constant field shows a smaller δQ than the same temperature model with a field strength decreasing with height, demonstrating the sensitivity of δQ to the magnetic field gradient, which we have not analysed in Sect. 2.2, and which is a result of the (probably) larger height of formation of the π-component than of the σ-components.

Note also that the two lines are not equally well reproduced, a slightly better fit being achieved for 5250.2 Å than for 5247.1 Å. This may be a result of the greater sensitivity of 5247.1 Å δQ to temperature, due to the smaller Landé factor of this line (cf. Sect. 2.2). As a comparison we have also carried out calculations with the network model of Solanki (1986). It gives lower δQ for both lines, and gives a reasonably good fit to 5247.1 Å, but a somewhat too small asymmetry for 5250.2 Å. All in all, the calculations suggest that for most regions the fluxtube temperature structure lies between that of the two models. However, with only two lines we cannot, due to noise induced scatter, decide whether the dependence of the fluxtube temperature on filling factor suggested by a few observations near disk center also holds for these regions observed closer to the limb. A statistical analysis will be required to decide this question.

3.5. Q/V-ratio and inclination

A number of authors have presented observational evidence, mostly of quite indirect nature, for tilted non-sunspot fields. Early indirect measurements include those of Stoyanova (1970) and Krat (1973). One of the rare direct measurements is that of Deubner (1975), who interpreted vector magnetograph data as suggesting an isotropic distribution of the inclination of field lines. Later Schoolman and Ramsey (1976) and Tarbell and Title (1977) presented some indirect and inconclusive evidence for almost horizontal fields in what they termed the 'dark component of the network'. From a comparison of magnetograms with Ca II plages Wiehr (1978) concluded that fluxtubes are inclined by 55° towards the west. Brants (1985) assumed that slanted fields are present when Stokes I of Fe I 6302.5 Å has a large width, but its Stokes V has only a small amplitude. However, alternative explanations can be proposed which are equally valid. For example a partial cancellation of opposite polarities in the resolution element (some evidence for such an effect on a spatial scale of 1″ has been presented by Koutchmy and Stellmacher, 1987), or the presence of regions with a particularly large velocity broadening. In contrast to these observations, theoretical models always assume fluxtubes to be vertical (e.g. Spruit, 1976; Deinzer et al., 1984; Pneuman et al., 1986; Steiner et al., 1986). Furthermore, Schüssler (1986) has demonstrated that their large buoyancy will hinder fluxtubes from assuming too large angles to the vertical.

In this section we set constraints on the angle of inclination of fluxtubes by comparing model calculations of Q/V with the data of Paper I. We compensate for the influence of magnetic field strength, turbulence velocity, and temperature in fluxtubes (which is not of critical importance, cf. Sect. 2.3) on Q/V by using our best estimates of these quantities.

The fit of the synthetic Q/V ratio to the data is illustrated in Fig. 11 (a: Fe I 5250.2 Å, b: Fe I 5247.1 Å). The solid curves are produced by the plage model with thin tube $B(\tau = 1) = 2000$ G magnetic field, as well as with $B = 1140$ G = constant. In this first step we have assumed that the fields are vertical (i.e. $\gamma_1 = \theta$, where γ_1 denotes the γ of the first step). We have also used a slightly different definition of Q/V than the one used in Sect. 2.3 [Eq. (16)]

$$\frac{Q}{V} = \frac{a_\sigma(Q)}{a_\sigma(V)} \frac{\mu}{1-\mu^2}. \tag{19}$$

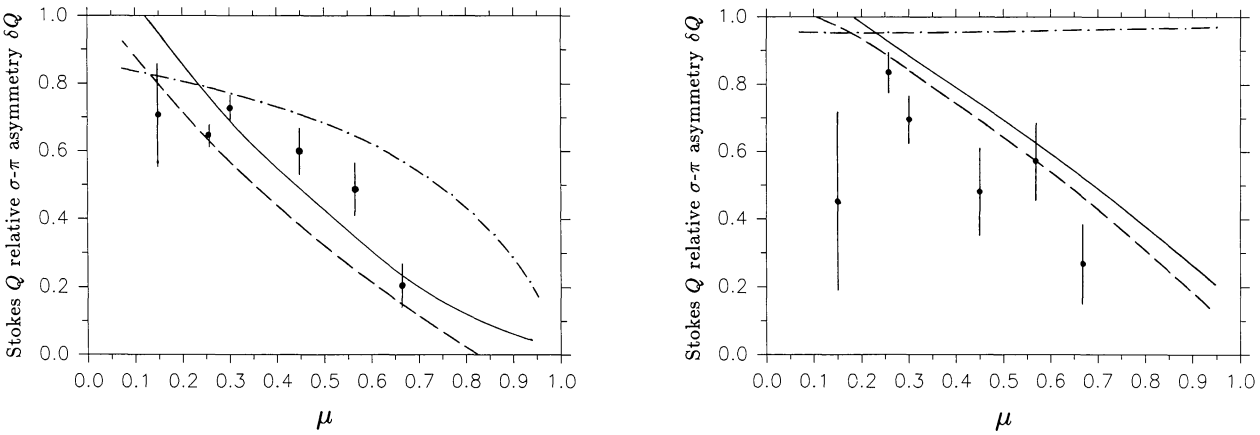

Fig. 10. δQ vs. μ. The models are the same as in Fig. 7b. **a** Fe I 5250.2 Å. **b** Fe I 5247.1 Å

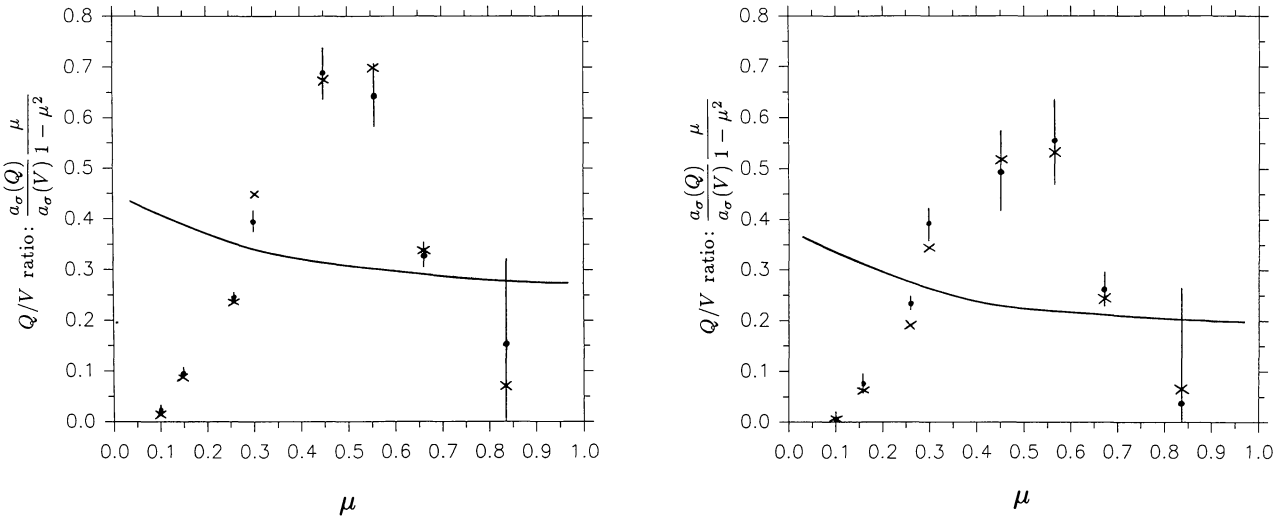

Fig. 11. $Q/V(\mu^2/(1-\mu^2))$ vs. μ. Filled circles: FTS data. Solid curves: Plage model with vertical field. Both, thin tube magnetic field with $B(\tau = 1) = 2000$ G and a constant field of strength 1140 G, give practically the same values. Crosses: Q/V ratio calculated assuming fields inclined to the vertical. **a** Fe I 5250.2 Å. **b** Fe I 5247.1 Å

The two definitions are identical for vertical fields ($\mu = \cos\theta = \cos\gamma$), but differ when this is no longer the case. Eq. (16) is more useful for test calculations, when we know γ, but Eq. (19) is better suited for observational data, since we do not know the γ for the observed regions in advance.

Evidently there is no correspondence between the data and the model calculations. Therefore, the CLV of the observed Q/V is not due to changes in line shape or field strength. Calculations with other field strengths and with the HSRA support this conclusion. The obvious remaining reason for the discrepancy is that the fields are not vertical. In a second step we have therefore determined the angle to the line of sight which the magnetic fields must have in order to reproduce the data, while keeping $\chi = 0°$. In the absence of Stokes U data this is the simplest choice for χ. To avoid lengthy calculations we assume that Q and V vary like their absorption coefficients with γ and χ, i.e.,

$$Q \sim \sin^2\gamma \cos 2\chi\,, \qquad (20)$$
$$V \sim \cos\gamma\,.$$

We then obtain the new γ, which we call γ_2, from a comparison of the measured ratio $(Q/V)_m$ with the ratio calculated in the first step $(Q/V)(\gamma_1, \chi = 0)$:

$$\left(\frac{Q}{V}\right)_m = \left(\frac{Q}{V}\right)(\gamma_1, \chi = 0)\frac{\sin^2\gamma_2}{\cos\gamma_2}\frac{\mu}{1-\mu^2}\,. \qquad (21)$$

Using this new γ_2 we again calculated the profiles and determine their $Q/V = (Q/V)(\gamma_2, \chi = 0)$ ratio.

The results of this second iteration are marked by crosses in Fig. 11. The main source of discrepancy between data and models is now the noise, which introduces some slight inconsistency ($< 5°$) between 5250.2 Å and 5247.1 Å. Whenever $\gamma_2(5250) \neq \gamma_2(5247)$ we have used the average value. The magnitude of the discrepancy due to the use of Eq. (20) is even smaller and a posteriori justifies our use of it. μ, θ and γ_2 are listed in the first three columns of Table 1. In order to calculate the angle of inclination, φ, of the fluxtubes with respect to the vertical direction in the atmosphere we require both γ and χ. Since, due to the absence of Stokes U data, we cannot measure χ, we can either determine φ by assuming some arbitrary χ value (e.g. $\chi = 0^0$, then $\varphi = |\gamma_2 - \theta|$), or we can test how strong the influence of different χ values is on φ. 45° is an upper limit for $|\chi|$, since Q disappears for this value and changes sign above it, something we do not observe. Of course, for $135° \leq |\chi| \leq 180°$ Stokes Q again assumes the same sign as for $45° > |\chi|$, but this simply corresponds to a reversal in magnetic polarity and does not affect φ. We determine the γ which gives the observed Q/V ratio for each χ on a grid with $0° \leq \chi \leq 40°$ from the following consideration. As we have seen, to a high order of accuracy

$$\frac{Q}{V}(\gamma_3, \chi_3) = C\frac{\sin^2\gamma_3}{\cos\gamma_3}\cos 2\chi_3\,, \qquad (22)$$

where C is a constant determined from step 2,

$$C = \frac{\cos\gamma_2}{\sin^2\gamma_2}\left(\frac{Q}{V}\right)_m\,. \qquad (23)$$

The aim is to find $\gamma_3(\chi_3)$ such that

$$\frac{Q}{V}(\gamma_3, \chi_3) = \left(\frac{Q}{V}\right)_m\,. \qquad (24)$$

Table 1

μ	θ	γ_2	$\varphi_{\min}$	$\varphi_{\max}$	Direction of minimum inclination
0.83	33.9	20.8	13.1	28.4	E
0.67	47.9	49.7	1.8	41.0	W
0.57	55.2	70.1	14.8	48.2	W
0.45	63.3	74.5	11.2	45.1	W
0.30	72.5	76.0	3.5	42.0	W
0.28	74.9	69.4	5.5	40.9	E
0.15	81.4	59.7	21.7	39.7	E
0.10	84.3	30.1	43.9	54.2	SE/NE

Combining Eqs. (22), (23), and (24) we obtain

$$\cos\gamma_3 = \frac{1}{2}\left(-\frac{\sin^2\gamma_2}{\cos\gamma_2\cos 2\chi_3} + \sqrt{\frac{\sin^4\gamma_2}{\cos^2\gamma_2\cos^2 2\chi_3} + 4}\right). \quad (25)$$

Note that as χ_3 is increased, γ_3 always changes so that it gets closer to 90°.

For a given (γ, χ) pair we can determine (φ, ψ), with φ being the angle of the fluxtube to the vertical and ψ being the direction of its tilt, measured from the plane containing the line of sight and the vertical to the atmosphere, from the following pair of equations

$$\cos\varphi = \sin\gamma\cos\chi\sin\theta + \cos\gamma\cos\theta,$$

$$\sin\psi = \frac{\sin\gamma\sin\chi}{\sin\varphi}. \quad (26)$$

We have assumed that the polarization measurement is carried out such that χ is measured from the same plane as ψ. This is the case for the present observations.

Of interest are the minimum and the maximum φ values thus determined. These are listed in columns 4 and 5 of Table 1. Interestingly, all the regions give $\varphi = \varphi_{\min}$ for $\chi = 0°$, except for the region nearest the limb for which $\varphi = \varphi_{\min}$ for $\chi = 40°$. Note that $\chi = 0°$ corresponds to $\psi = 0°$, or 180°, depending on the sign of Stokes V, while for the region nearest the limb $\psi(\varphi_{\min}) \approx \pm 55°$, the uncertainty in sign being due to the lack of Stokes U information. Since the observations were all carried out near the solar equator, $\psi = 0°$ corresponds to approximately the E or W direction on the Sun. The approximate direction of minimum inclination is listed in column 6 of Table 1. Note that we have not taken the changing influence of the magnetooptical effects into account in this last step. However, since the σ-amplitudes of both Q and V are relatively unaffected by magnetooptical effects for the magnetic field strengths found in fluxtubes we need not worry about them further.

How significant are these φ values? From Fig. 11 we see that the error bars are quite small, except for the observation at $\mu = 0.83$. We therefore conclude that the fluxtubes in the regions at $\mu = 0.57, 0.45, 0.15$, and 0.10 *averaged over* $(5'')^2$, must be inclined by more than 10° to the normal. A more detailed discussion on the possible interpretations of this result is given in Sect. 4.

3.6. *Second iteration*

After having gone through the complete procedure, as described in Sects. 3.1 to 3.5, we can return to the beginning and start anew, now using the fluxtube parameters obtained during the first iteration as input. In practice we find, however, that most properties remain unchanged during the second iteration. A notable exception is the 5250/5247 Stokes V line ratio. Its considerable γ dependence means that for regions with inclined fields the line ratio is somewhat changed. Fortunately, the change is always such that the models now provide a better fit to the data with the same magnetic field as before. Thus some of the scatter of the observed V ratio is due to the inclination of the fields and only a part is due to the filling factor, whose influence has been stressed in Paper I. A future improved version of the regression equation applied to the CLV of the 5250/5247 Stokes V line ratio in Paper I would therefore have to incorporate both influences. Since the filling factor does not influence any of the other steps of the procedure (for a simple 2-component model), but its determination is itself influenced by most of the other fluxtube properties, we determine it separately at the end.

3.7. *Stokes V amplitude and filling factors*

The simplest and at the same time most often used method of deriving the (relative) filling factor is to simply suppose $\alpha \sim a(V)$, where $a(V) = 1/2(a_b(V) + a_r(V))$. Obviously, this interpretation has certain problems. Firstly, $a(V)$ is temperature, field strength and velocity dependent. This is particularly true for low excitation Fe I lines like the often used 5250.2 Å line. Thus variations in these quantities from one region to another (or at different μ values) will also affect the determined α. Secondly, the presence of inclined fields or of a mixture of polarities in the resolution element will also completely distort the α value (note that telescope depolarization will act like a partial cancellation of polarities). Thirdly, as pointed out by Grossmann-Doerth et al. (1987) and Schüssler and Solanki (1987), all methods of determining α actually only deliver $\alpha\delta_c$, where δ_c is the ratio of the continuum intensity of the fluxtube to that of the quiet sun.

In this section we attempt to determine the filling factors of the regions we have studied so far, while taking the above caveats into account as completely as possible. Let $a^{\text{calc}}(\gamma, B, T, \xi, \mu)$ be the amplitude of the Stokes V profile calculated using our best estimates for the fluxtube parameters in a particular region, and $a^{\text{obs}}(\mu)$ the observed V amplitude of the same line in that region. Both a^{calc} and a^{obs} are normalised relative to the local continuum. Then α is given by

$$\alpha = \frac{a^{\text{obs}}(\mu)}{\delta_c(\mu)a^{\text{calc}}(\gamma, B, T, \xi, \mu)}. \quad (27)$$

Table 2 lists μ, a^{obs}, $a^{\text{calc}}(\gamma_2)$, $\alpha(\gamma = \theta)\delta_c$, $\alpha(\gamma_2)\delta_c$, δ_c, and α, respectively. Some of the numbers require further elucidation. a^{obs} and a^{calc} refer to Fe I 5247.1 Å. We have used the plage model for all the calculations except for the two network regions at $\mu = 0.98$ and 0.83, where we have used the network model. The listed values of a^{calc} are based on the γ_2 values (i.e. γ determined assuming $\chi = 0°$, which for most regions gives $\varphi = \varphi_{\min}$) for the eight regions for which we have Stokes Q measurements, while for the other two regions we have assumed vertical fields. For these two regions we have also multiplied a^{obs} by a factor of two to account for the calibration error discovered by Stenflo and Harvey (1985). We have also derived $\alpha\delta_c$ by taking a^{calc} values calculated using $\gamma = \theta$. These are listed in column 4. $\delta_c(\mu)$ has been observed with high resolution in white light by Muller (1975). However, his disk centre contrast of 1.05 is considerably smaller than the lower limit of 1.4 set from an analysis of FTS Stokes I spectra by Schüssler and Solanki (1987). This difference is probably due to the fact that Muller could not resolve the fluxtubes despite a spatial resolution superiour to 0.5″. If, as a crude estimate, we assume that the ratio of fluxtube diameter to resolution element remains unchanged when μ decreases (the exact dependence is a function of the detailed geometry of the fluxtube; e.g. if hot walls or a hot cloud give rise to the continuum contrast), then we obtain a lower limit to the true $\delta_c(\mu)$ by multiplying Muller's observed function by 1.4. This somewhat questionable procedure results in the δ_c values in column 6 of Table 2.

By comparing columns 4, 5, and 7 in Table 2 we see the importance of a proper determination of γ (columns 4 and 5) and $\delta_c(\mu)$ (columns 5 and 7). In particular for the region at $\mu = 0.1$

Table 2

μ	$a^{obs}(V)$ %	$a^{calc}(\gamma_2)$ %	$\alpha(\gamma=\theta)\delta_c$	$\alpha(\gamma_2)\delta_c$	δ_c	α %
0.98	0.96	8.54	0.11	0.11	1.49	7.5
0.92	5.44	13.90	0.39	0.39	1.54	25.4
0.83	0.94	7.82	0.12	0.11	1.62	6.6
0.67	4.37	10.56	0.41	0.43	1.68	25.5
0.57	1.04	9.43	0.12	0.18	1.77	10.4
0.45	1.86	8.73	0.21	0.36	1.87	19.1
0.30	1.65	5.58	0.30	0.37	2.05	17.9
0.28	3.09	4.84	0.64	0.47	2.05	23.0
0.15	1.92	2.68	0.72	0.21	1.92	11.1
0.10	3.23	1.66	1.95	0.23	1.78	12.9

the $\alpha\delta_c$ value drops from a rather improbable 1.95 to a more realistic 0.23 when the inclination is taken into account.

Our α values are, however, still susceptible to fault. Besides the fact that the simple multiplication of Muller's $\delta_c(\mu)$ by a factor of 1.4 may be considerably wrong, there is always the possibility that the individual regions do not all have the same temperature. We actually know that there is a difference between the regions at $\mu = 0.98$ and 0.92. A spectral line cannot be simultaneously both a good diagnostic of temperature and of filling factor. Our chosen lines are good diagnostics of temperature. Here we see the limitations of the few-lines techniques. However, we can easily improve the relative α values by adding a third line less sensitive to temperature, e.g. Fe II 5197.6 Å.

Another effect which could lead to errors in $\alpha\delta_c$ was discovered by Van Ballegooijen (1985b), who found that if the small width of the narrowest fluxtubes is taken into account, then the Stokes V signal decreases rapidly as soon as they are no longer observed along their axis of symmetry. This would lead to an underestimation of $\alpha\delta_c$ for regions with large γ.

Finally, we see a significant correlation between the value of α in column 7 of Table 2 and $a^{obs}(V)$. This may be the result of correlations between some of the parameters on which α depends [listed in Eq. (27)]. Possible sources are our procedure for selecting the observed regions (see Paper 1), the method of calculating α, chance, or a deeper relationship between the various parameters. Only future observations can decide between these possibilities.

4. Discussion and conclusions

We have presented a procedure based on model calculations for deriving many of the basic parameters of solar magnetic fluxtubes with a minimum of a priori assumptions. Before applying this procedure to the data we have analytically and numerically investigated some of the diagnostic techniques used, in order to explore their weaknesses and strengths. As a byproduct we have demonstrated that whereas the integrated Stokes V profile is an approximation of Stokes I for all lines having sufficiently small Zeeman splitting this is true for the doubly integrated Stokes Q and U profiles only in the case of very weak (i.e. saturation free) lines.

Application of the procedure to the data allows us to improve the constraints on the field strength in fluxtubes. It also shows that the CLV of the 5250/5247 V and Q line ratios contains only very limited information on the height variation of the magnetic field. Both a constant magnetic field and a field strength decreasing with height can reproduce the data equally well. This is partly due to a dependence of the line ratio on γ induced by the increasing importance of the π-component with increasing γ. If we use the thin tube approximation, then a magnetic field with $B(\tau = 1) = 2000$ G gives the best fit to the data (note that at $\tau = 10^{-2}$ the field strength has dropped to approximately 1000 G). We also notice that the velocity broadening affects the line ratio and thus the deduced field strengths considerably. For the turbulence velocity we obtain values directly from Stokes V similar to those that Solanki (1986) obtained from the I_V profile. For the two lines investigated the total turbulent velocity does not appear to decrease with increasing γ, as would be expected if the mass-motions were restricted to the direction parallel to the field lines. We also find that the models of Solanki (1986) give a CLV of the Q asymmetry, which is in reasonable agreement with the observations, although an improvement of the temperature structure might still be needed.

From the Q/V ratio we determine lower limits for the inclination of the fluxtubes. We find that half of the regions observed have fluxtubes inclined by at least 10° to the normal. A theoretical understanding of this result appears problematic at the moment, since the highly evacuated fluxtubes are expected to stay vertical due to buoyancy (Schüssler, 1986). Although motions in their surroundings may lead (small) individual fluxtubes to deviate substantially from the vertical, we would expect a larger sample of fluxtubes, such as those within an area of $(5'')^2$, to be on the average more or less vertical. Since the observations were carried out in strong active region plages, it is possible that strong sunspot fields (low lying canopies, Giovanelli and Jones, 1982) may, by pushing the fluxtubes towards one side, be the cause of the inclination, since magnetic tension would lead the lower layers to be also slightly inclined. Future observations of all four Stokes parameters may be able to test this hypothesis by deriving the magnitude and direction of inclination as a function of position relative to sunspots. However, this explanation is probably not sufficient for the region at $\mu = 0.1$. It has by far the largest angle of inclination ($\varphi > 40°$) and is also the only region which shows signs of a sizeable downflow (cf. Fig. 7 of Paper I). This suggests that it may be a region of emerging flux, where we see only the newly emerged top of a loop.

Unlike Wiehr (1978) we are unable to find any preferred direction of inclination. However, we do not wish to comment further on Wiehr's finding since our observed sample is small and may not be quite free of bias from the method of selecting the regions to be observed (see Paper I). The method of selection may also have biased our sample to contain a high percentage of regions with a large inclination.

We have assumed so far that the fluxtubes are preferably inclined in a given direction. However, a field with a spread of inclinations such that all ψ values are equally present, for example the field of a cylindrically symmetric fluxtube which expands with height, also affects Q/V. Since such a geometry can only reduce the Q/V ratio, it simulates a magnetic field inclined towards the observer. Therefore, we expect models which take the expansion of fluxtubes into account to give somewhat smaller angles of inclination to the vertical for the three regions nearest the limb, but to result in more strongly inclined fluxtubes for the regions with $0.3 \leq \mu < 0.7$. Another effect which may influence the determined inclinations is the presence of a mixture of polarities in the resolution element. Such a mixture decreases Stokes V, but does not affect Stokes Q. It would therefore lead to an increase in the observed Q/V ratio, thus simulating a field inclined away from the observer. To what extent these two effects could account for the observations appears unclear.

We have also demonstrated the importance of the inclination of the field and the continuum contrast of the fluxtubes for the determination of the filling factor in support of the conclusions of Grossmann-Doerth et al. (1987) and Schüssler and Solanki (1987).

The fact that the CLV of the 5250/5247 line ratio cannot set constraints on the height variation of the magnetic field raises the question whether there are other possible methods of obtaining such information reliably. One possibility is the CLV of the infrared (IR) Fe I line at 15648.5 Å. Stenflo et al. (1987b) find a decrease of the magnetic field strength with height directly from the splitting of this line, although radiative transfer calculations are required to ascertain the reliability of this finding. There are also other indicators which suggest that the field strength really does decrease with height. An example is the comparison of the fields derived at *disk centre* from the IR line (1400 G) and in the visible (1000–1200 G). Since the IR line is formed deeper in the atmosphere than the lines in the visible (due to a minimum in continuum opacity near 1.6μ), this amounts to a height gradient as well. At disk centre the π-component should not play a major role for Stokes V, unless the fields are strongly inclined. Another possible technique of deriving the gradient of the magnetic field over a limited height range is from the 5250/5247 line ratio of the complete Stokes V profile, as has been outlined by Stenflo (1984). The magnetic field gradient may also be determined by comparing the 5250/5247 line ratio in the σ and π components of Stokes Q, since the π-component is formed higher in the atmosphere. This method has the advantage that we can obtain the gradient at a height not attainable with the V profile, since $V = 0$ at the centre of the line.

Finally, we wish to point out that this investigation has three main shortcomings. Firstly, being based on only two lines, it cannot achieve the generality of a many-lines analysis. Secondly, the radiative transfer limited to one line of sight, which reproduces the line profiles near disk centre quite well, is probably of less value closer to the limb. Thirdly, the missing Stokes U parameter is invaluable for deciding the true inclinations and therefore also the filling factors. Future improvements must focus on these three points: An analysis based on more spectral lines, 1.5-D radiative transfer, and simultaneous observations of all four Stokes parameters.

References

Beckers, J.M.: 1969a, *Solar Phys.* **9**, 372

Beckers, J.M.: 1969b, *Solar Phys.* **10**, 262

Blackwell, D.E., Ibbetson, P.A., Petford, A.D., Shallis, M.J.: 1979, *Monthly Notices Roy. Astron. Soc.* **186**, 633

Brants, J.J.: 1985, *Solar Phys.* **98**, 197

Calamai, G., Landi Degl'Innocenti, E., Landi Degl'Innocenti, M.: 1975, *Astron. Astrophys.* **45**, 297

Deinzer, W., Hensler, G., Schüssler, M., Weisshaar, E.: 1984, *Astron. Astrophys.* **139**, 435

Deubner, F.L.: 1975, *Osserv. Mem. Oss. Astrofis. Arcetri* **105**, 39

Dollfus, A.: 1958, *Comptes Rendue* **246**, 3590

Frazier, E.N., Stenflo, J.O.: 1978, *Astron. Astrophys.* **70**, 789

Gingerich, O., Noyes, R.W., Kalkofen, W., Cuny, Y.: 1971, *Solar Phys.* **18**, 347

Giovanelli, R.G., Jones, H.P.: 1982, *Solar Phys.* **79**, 267

Grossmann-Doerth, U., Pahlke, K.D., Schüssler, M.: 1987, *Astron. Astrophys.* **176**, 139

Harvey, J.W., Livingston, W.: 1969, *Solar Phys.* **10**, 283

Harvey, J.W., Livingston, W., Slaughter, C.: 1972, in *Line Formation in the Presence of Magnetic Fields*, High Altitude Observatory, Boulder, CO, p. 227

Holweger, H., Gehlsen, M., Ruland, F.: 1978, *Astron. Astrophys.* **70**, 537

Krat, V.A.: 1973, *Solar Phys.* **32**, 307

Koutchmy, S., Stellmacher, G.: 1978, *Astron. Astrophys.* **67**, 93

Landi Degl'Innocenti, E., Calamai, G.: 1982, *Astron. Astrophys. Suppl. Ser.* **49**, 677

Leroy, J.-L.: 1962, *Ann. Astrophys.* **25**, 127

Mathys, G., Stenflo, J.O.: 1987, *Astron. Astrophys.* **171**, 368

Muller, R.: 1975, *Solar Phys.* **45**, 105

Pneuman, G.W., Solanki, S.K., Stenflo, J.O.: 1986, *Astron. Astrophys.* **154**, 231

Rachkovsky, D.N.: 1967, *Izv. Krymsk. Astrofiz. Observ.* **37**, 56

Schoolman, S.A., Ramsey, H.E.: 1976, *Solar Phys.* **50**, 25

Schüssler, M.: 1986, in *Proc. Workshop on Small Magnetic Flux Concentrations in the Solar Photosphere*, W. Deinzer, M. Knölker, H.H. Voigt (Eds.), Vandenhoeck & Ruprecht, Göttingen, p. 103

Schüssler, M., Solanki, S.K.: 1987, *Astron. Astrophys.* (in press)

Semel, M.: 1986, in *Proc. Workshop on Small Magnetic Flux Concentrations in the Solar Photosphere*, W. Deinzer, M. Knölker, H.H. Voigt (Eds.), Vandenhoeck & Ruprecht, Göttingen, p. 39

Simmons, G.J., Blackwell, D.E.: 1982, *Astron. Astrophys.* **112**, 209

Solanki, S.K.: 1986, *Astron. Astrophys.* **168**, 311

Solanki, S.K.: 1987a, in *Proc. Workshop on The Role of Fine-Scale Magnetic Fields on the Structure of the Solar Atmosphere*, Tenerife, 6–12 Oct. 1986, in press

Solanki, S.K.: 1987b, Ph.D. *Thesis*, E.T.H., Zürich

Solanki, S.K., Stenflo, J.O.: 1984, *Astron. Astrophys.* **140**, 185

Solanki, S.K., Stenflo, J.O.: 1985, *Astron. Astrophys.* **148**, 123

Solanki, S.K., Stenflo, J.O.: 1986, *Astron. Astrophys.* **170**, 120

Spruit, H.C.: 1976, *Solar Phys.* **50**, 269

Steiner, O., Pneuman, G.W., Stenflo, J.O.: 1986, *Astron. Astrophys.* **170**, 126
Stenflo, J.O.: 1973, *Solar Phys.* **32**, 41
Stenflo, J.O.: 1975, *Solar Phys.* **42**, 79
Stenflo, J.O.: 1984, *Adv. Space Research* **4**, 5
Stenflo, J.O.: 1985, in *Measurements of Solar Vector Magnetic Fields*, M.J. Hagyard (ed.), NASA *Conf. Publ.* **2374**, 322
Stenflo, J.O., Harvey, J.W.: 1985, *Solar Phys.* **95**, 99
Stenflo, J.O., Harvey, J.W., Brault, J.W., Solanki, S.K.: 1984, *Astron. Astrophys.* **131**, 333
Stenflo, J.O., Solanki, S.K., Harvey, J.W.: 1987a, *Astron. Astrophys.* **171**, 305 (Paper I)
Stenflo, J.O., Solanki, S.K., Harvey, J.W.: 1987b, *Astron. Astrophys.* **173**, 167
Stoyanova, M.N.: 1970, *Solar Phys.* **15**, 349
Tarbell, T.D., Title, A.M.: 1977, *Solar Phys.* **52**, 13
Title, A.M., Tarbell, T.D.: 1975, *Solar Phys.* **41**, 255
Unno, W.: 1956, *Publ. Astron. Soc. Japan* **8**, 108
Van Ballegooijen, A.A.: 1985a in *Measurements of Solar Vector Magnetic Fields*, M.J. Hagyard (ed.), NASA *Conf. Publ.* **2374**, 322
Van Ballegooijen, A.A.: 1985b, in *Theoretical Problems in High Resolution Solar Physics*, H.U. Schmidt (Ed.), MPA, Munich, p. 167
Wiehr, E.: 1978, *Astron. Astrophys.* **69**, 279